NASA Technical Memorandum 83352

A Comprehensive Analysis of Cavitation and Liquid Impingement Erosion Data

P. Veerabhadra Rao and S. G. Young
Lewis Research Center
Cleveland, Ohio

Prepared for the
Second Conference on Cavitation
sponsored by the Institution of Mechanical Engineers
Edinburgh, Scotland, September 6–8, 1983

NASA

P VEERABHADRA RAO and S G YOUNG
National Aeronautics and Space Administration
Lewis Research Center
Cleveland, Ohio 44135
A Comprehensive Analysis of Cavitation and Liquid Impingement Erosion Data

A COMPREHENSIVE ANALYSIS OF CAVITATION AND LIQUID IMPINGEMENT EROSION DATA

P. Veerabhadra Rao and S. G. Young

National Aeronautics and Space Administration
Lewis Research Center
Cleveland, Ohio 44135

SYNOPSIS Cavitation-erosion experimental data previously reported by the present authors covering several materials tested in a rotating disk device and a magnetostriction apparatus have been analyzed using normalization and curve-fitting techniques. From this process a universal approach is derived which can include data from cavitation and liquid impingement studies for specific materials from different test devices.

1 INTRODUCTION

One of the primary objectives of erosion research has been to model laboratory erosion data to field conditions with more confidence and reliability. Honegger (1), as early as 1927, considered "specific erosion" in an attempt to compare materials and time effects. However, systematic investigations pertaining to time effects on erosion rates were conducted in the mid-1960's (2 to 5). In view of the strong dependence of the erosion rate on exposure time in both cavitation and liquid impingement environments, several formulations, models, nomograms, and charts were presented by different investigators (4 to 14). The main purpose of these formulations was to

(a) Identify the damage as well as erosion mechanisms involved during the erosion process with time;

(b) Characterize and quantify, as precisely as possible, the erosion rate as the exposure time increases for long terms;

(c) Test less resistant materials in the laboratory for relatively short times and extrapolate these data to resistant materials in the field.

In view of the difficulties encountered in the past to characterize and model materials with different devices and laboratory conditions, many investigators agree that comparisons of test results should be done only if based on the corresponding stages of the erosion-rate-versus-time curves. Specifically, these stages have been named the incubation period, the acceleration period (accumulation zone), the peak damage rate, the deceleration period (attenuation zone), the steady-state region, and the long-term erosion period, which is characterized as either cyclic, decreasing, or increasing, depending on the test method and the erosion resistance of the material (15). Typical erosion-rate-versus-time curves are reproduced in Fig. 1 depicting all periods (2 to 5).

A historical background of work on long-term cavitation erosion prediction and methods for modeling the erosion-rate-versus-time curves are presented in a recent study by the authors (16). Several prediction equations for liquid impingement erosion are presented in (15). The important models, formulations, nomograms, and the variables necessary to evaluate the erosion-versus-time curve or erosion in a certain amount of exposure time are presented in Table 1. No single model or prediction attempt has yet been fully precise in its ability to predict erosion rates either during the initial phases of damage or during the advanced stages of erosion. Hence, long-term predictions using earlier formulations differed from actual data by factors of two or more. Most prolonged operations of machines require a higher confidence level to operate machinery at optimum efficiency. Thus if a method is devised to accurately predict the long-term erosion of a baseline material, and it is found that the predicted erosion would be detrimental, either the material may be changed at the design stage or more accurate overhaul periods may be established.

A method for erosion-rate-data curve fitting is presented as normalized cumulative average erosion rate as a function of normalized time. This method greatly reduces individual variations of the instantaneous-erosion-rate-versus-time curves. In this manner, a universal approach to the analysis of data from previous experimental results is presented for prediction purposes. The long-term exposure behavior is discussed and correction factors pertaining to the incubation period are described. This paper is a condensed version of (16).

2 NOTATION

ER	erosion rate
MER	maximum erosion rate
p	pressure
t	exposure time to cavitation or impingement erosion
$t_a, t_b, t_c, \ldots t_n$	incubation periods of curves in A,B,C,...N in Fig. 9
t_i	incubation period of a typical erosion-rate-versus-time curve

t_m	time to attain maximum or peak rate of erosion on rate-versus-time curves
V	velocity
V	cumulative volume loss due to cavitation erosion corresponding to t hours exposure
V_m	maximum cumulative volume loss due to cavitation erosion corresponding to the slope of the erosion-versus-time curve joining the origin and the point of tangency
Δt	incremental time causing an incremental volume loss ΔV
ΔV	incremental volume loss of material in incremental time Δt

Subscripts:

a	cumulative average
i	instantaneous

3 DATA ANALYSIS AND PROCEDURE

3.1 Erosion Data Sources

In the development of this curve-fitting approach for long-term cavitation erosion-rate prediction, original data sets obtained independently by each of the present authors were used. One used a rotating disk device (17) and the other a magnetostriction apparatus (18 to 20). The details of the rotating disk device and magnetostriction apparatus have been described in detail in (19, 21, and 22).

The experimental conditions for the rotating disk device were velocity, 35 to 37.3 m/s; pressure, 0.11 to 0.17 MPa (abs); diameter of the cavitation inducer, 25.4 mm; and test liquid, water. The materials tested were aluminum, copper, brass I, brass II, stainless steel, and mild steel. The compositions of materials and their properties were reported in (16, 21, and 22). The experimental conditions pertaining to the magnetostriction apparatus were frequency, 25 kHz; amplitude, 44 μm; test liquids, sodium (from 204° to 649° C), and water. The materials tested were nickel, aluminum, zinc, iron, L-605 cobalt-base alloy, Stellite, and stainless steel; the compositions of materials and their mechanical properties were previously reported (18 to 20).

3.2 Erosion Data Treatment Method

Figure 2 presents cumulative-erosion-versus-exposure-time curves for stainless steel tested in a rotating disk device at four different velocities (17). Figure 3(a) presents instantaneous-erosion-rate-versus-time curves for the same material (see upper curve in Fig. 2). As erosion resistance increases the incubation period becomes more pronounced. Because there are several peaks and valleys in the erosion-rate-versus-time curves, the prediction of erosion rate with exposure time becomes increasingly difficult.

As a first step to improve the situation, the cumulative average erosion rate is calculated and plotted versus time (Fig. 3(b)) for the same data presented in Fig. 2. The oscillations observed in Fig. 3(a) are considerably smoother in Fig. 3(b) because of this treatment. It is now evident that a material responds to erosion in a similar manner at different velocities and each erosion-rate-versus-time curve has a maximum erosion rate if the test has been run for a sufficient length of time.

Using these similarity principles, each data point of Figs. 3(a) and (b) was normalized with respect to peak erosion rate and the time corresponding to this peak. Figures 4(a) and (b) present normalized-instantaneous-erosion-rate-versus-normalized-time and normalized-cumulative-average-erosion-rate-versus-normalized-time, respectively. However, the scatter in Fig. 4(a) is too great to provide an accurate curve or predictive equation for the field engineer. Theoretical and empirical models proposed by earlier investigators (Table 1) do not fit these plots unless many assumptions are made; furthermore, the scatter bands are large (16). On the other hand, Fig. 4(b) provides a smooth curve without oscillations, indicating that a properly normalized erosion rate follows a certain natural trend even under different experimental conditions.

4 RESULTS AND DISCUSSION

Figure 5 presents typical normalized cumulative erosion rate versus normalized time for different materials tested in a rotating disk device and a magnetostriction apparatus using both vibrating and stationary specimens. A comparison of normalized-instantaneous-erosion-rate-versus-normalized-time curves for the same materials (16) indicated that there is too much scatter and most of the individual materials cannot be represented by any single formulation. Figure 5, on the other hand, shows a considerable reduction in scatter. This consistent configuration was observed not only for materials tested in a rotating disk device with water, but also for a variety of materials tested with a magnetostriction device using both water and liquid sodium.

The ratio of instantaneous/cumulative peak heights MER_i/MER_a varied from 1.0 to 3.87 for materials tested in the rotating disk device and from 1.0 to 1.71 for materials tested with the magnetostriction apparatus using water and liquid sodium (16). As would be expected, the times to attain maximum cumulative erosion rate (tm_a) were always longer than the times to attain maximum instantaneous erosion rate (tm_i). Furthermore, for the materials tested, the ratio tm_i/tm_a varied from 0.42 to 0.960 in the rotating disk device and from 0.3 to 0.88 in the magnetostriction apparatus (16). As the erosion resistance of the material increased, the ratio MER_i/MER_a decreased. No clear-cut trend for the ratio tm_i/tm_a was observed.

The advantages of normalized-cumulative-erosion-rate-versus-normalized-time plots are (a) scatter of the instantaneous-erosion-rate-versus-time curves is greatly reduced, resulting in a consistent, relatively smooth set of curves; and (b) the MER_a and tm_a can be evaluated from the erosion-versus-time curve.

4.1 Comparisons with Earlier Investigations

Data reported by Kerr (23), Thomas and Brunton (24), and Elliott, et al. (25) were analyzed in the same manner as the present investigations

(16); typical plots are presented in Fig. 6. The improvement of using cumulative erosion rate was clear for data reported in (23, 24). This data treatment further supports the view that the normalized cumulative-erosion-rate-versus-time curves have significant advantages for erosion prediction with reduced data scatter. It was noted from Figs. 5 and 6, the quantitative data in (16), and the typical data in Table 2 that brass and stainless steel tested at different experimental conditions agreed very well on the normalized average basis. Results in Table 2 indicate that MER_i/MER_a varied from 1.4 to 3.2 and tm_i/tm_a from 0.68 to 0.82. One may therefore infer that quantitative correlations exist between cavitation and liquid impingement irrespective of the type of device used to produce erosion.

4.2 Effect of Time Increments on Prediction Models

"How many experimental points are necessary?" and "What time intervals should be used to obtain the most precise predictions possible?" are frequently asked questions. To investigate the effect of the interval length on the accuracy of the final plots, Fig. 7 was plotted using 1-hr intervals for cavitation data of the cobalt-base alloy L-605 in liquid sodium at 427° C. The same data with time intervals of 5, 10, and 15 min are presented in Fig. 5(b). With fewer points the determination of maximum erosion rate and tm is affected as shown in Table 3.

Major differences can be noted by comparing the two sets of data. The parameters calculated at 60-min intervals are far less accurate than those calculated at 5-, 10-, and 15-min intervals. Errors of 50 to 300 percent were observed in determining the parameters MER_a and tm_a. As the erosion resistance decreased, the error increased with long interval experiments (Table 3). Figures 5(b) and 7 indicate, however, that these close-interval data need be collected only until an accurate peak is attained. Since MER_a and tm_a are the crucial parameters which are used to calculate the requisite quantities, errors involved in their determination will lead to greater inaccuracies when they are used for long-term predictions. This study points out the importance of using close intervals in the early stages of erosion (up to the peak rate of erosion) to arrive at precise parameters for prediction purposes.

4.3 Effect of Long Exposure on Erosion Rates

The long-term erosion rate has been controversial ever since investigators have been aware of the influence of test time on erosion rate. Some investigators have reported continuous decrease in erosion rate after the initial peak rate, some have reported constant final rates (steady state), while others report cyclic rates at even longer exposures. All of these patterns have been well documented in (2 to 7) and in various papers presented at the ASTM symposia (26 to 29). Cumulative-erosion-rate-versus-time curves are presented in Fig. 8 in the normalized form, which generally shows a decreasing trend irrespective of erosion resistance and material (17 to 19).

The long-term exposure plots presented in Fig. 8 are unique, as the ratio t/tm_a approached nearly 400 (the highest ratio believed to be observed to date). Some of the deviations from a smooth curve in these plots are believed to result from the small number of data points taken during the incubation and acceleration periods. As explained in the previous section, difficulties in obtaining the true values of MER_a and tm_a and the sensitivity of these parameters to good long-term predictions are partially responsible for the difficulty in obtaining a single plot.

4.4 Incubation Period Correction

A typical set of most commonly observed cumulative-erosion-rate-versus-time curves is schematically represented in Fig. 9(a). The incubation periods are indicated in the figure as t_a, t_b, and t_c. By subtracting these times from the time of each experimental point on each of the respective curves, a condensed set of plots is generated (Fig. 9(b)). The new normalized time for peak erosion rate is now calculated as $(t - t_i)/(t_m - t_i)$.

All plots of normalized cumulative erosion rate and normalized time use the relationships $(V/t)/(Vm/tm)$ and t/tm, respectively. A correction factor for incubation period as used in Fig. 9(b) is necessary for all the previous figures; this correction factor would shift the curves toward the y-axis by the amount of time equivalent to the incubation period. In making the transition from the model to prototype the incubation period for the prototype relative to the model should be known in order to make this correction for more accurate long-term predictions.

Recently Heymann (30), while analyzing the ASTM G-2 sponsored 'round robin' test program, found that comparisons and correlations with the (maximum) cumulative erosion rate gave more scatter and inconsistency than those using maximum instantaneous erosion rate. This is primarily because the incubation period is dependent on the average erosion rate, and because there is more scatter in incubation periods than in maximum erosion rates (30). A possible disadvantage of the incubation period correction suggested is that it may sometimes remove one of the fundamental definition of the average-erosion-rate approach. Some investigators (e.g., 31 and 32) used incubation period to predict erosion rates. These correlations are better than material property correlations with erosion rates (32). (Neither of these investigators (31, 32) considered long-term erosion-rate predictions.)

4.5 Erosion Resistance Variation

Laboratory and field devices produce uneven erosion over the test specimen; hence, calculations for erosion resistance are very general and vary considerably even within the same device or test.

The normalized cumulative erosion-rate-versus-time curves in the present investigations, though generally smooth, indicate some deviations with erosion intensity. As the erosion resistance decreased, the portions of the curves following the peaks attained a lower value at long test times. For a single test device these portions of the curves were lower at long times for more resistant materials. But the height of each curve at longer test times appears to be a function of both the device and the material. This correlation between the level of the long-term-erosion-rate-versus-time curve and erosion resistance may be helpful in applying this universal plot approach to data from both laboratory and field devices. An empirical factor called 'the apparatus severity factor' is described in (15) for liquid impingement data. This may serve as an alternate approach to this discussion.

4.6 Universal Approach Plots

Summary plots of normalized erosion rate versus normalized time are presented in Fig. 10 for the previous experimental data from brass, stainless steel, mild steel, and cobalt alloy L-605. Every material tested in any type of cavitation or liquid impingement device can be represented in this manner. Depending upon the test device and material tested, a mean curve may be chosen and scatter bands can be defined or derived. The accuracy of the derivation of the two parameters tm_a and MER_a (including the incubation period) contributes to the accuracy of the prediction. The deviation is greater in the normalized time region from 0 to 1 than it is in any other portion of the curve.

Although the plots of Fig. 10 are similar to the set of plots reported by another investigator (7), Fig. 10 is based on experimental data without any assumptions or direct relation to theory. The plots in (7) were generated using instantaneous erosion rate versus time while the present curves of Fig. 10 were developed using cumulative erosion rate versus time. Equations proposed in (9) use both tangent points and fixed average-depth-of-erosion values combined with a curve-fit approach which results in much wider variations than in the current study.

The concept of a normalized-cumulative-erosion-rate-versus-normalized-time curve was first suggested by Heymann (9) and used by one of the present authors (17, 22) to check the validity of the erosion theory proposed by Thiruvengadam (7) for a rotating disk device. By using cumulative erosion rate instead of instantaneous erosion rate the data scatter was considerably reduced, and the plots (22) were closer to the theoretical curves presented in (7). The use of cumulative erosion rate was also considered by Lichtarowicz (12). Normalized-instantaneous-erosion-rate-versus-normalized-time curves have also been presented for erosion-corrosion modeling using a magnetostriction apparatus (33) and for steam turbine blade and shield materials using four different impingement devices (25). Lichtarowicz (12) also suggested that only two parameters MER_a and tm_a may be used to predict cumulative erosion rates for aluminum (Table 1). However, this paper shows the importance of two additional parameters, the incubation period t_i and the erosion resistance (1/ER).

The erosion process due to cavitation and liquid impingement is believed to be a function of the earlier history of the eroded surface (including work hardening, surface stresses, and changes in material properties). Also, a study of the relationship between the surface roughness and the erosion rate would be helpful to gain additional insight into the erosion process at longer times.

4.7 Application of the Universal Curve Fit Approach

To check the advantage of the analysis proposed in this paper, data reported in (25) for stainless steel during liquid drop impingement at a velocity of 305 to 314 m/s were analyzed. Of the three devices used, the English Electric Company (EEC) data have been taken as standard and normalized time as 2. Table 4 presents the parameters of MER_i, tm_i, MER_a, tm_a, and percentage error measured while analyzing instantaneous and cumulative erosion rate. In most situations, cumulative erosion rate provides a better prediction than instantaneous erosion rate. It is then possible to calculate the theoretical cumulative erosion of a specimen at any point in time. This information is useful in determining the extent of a component's erosion and its remaining useful life.

5 CONCLUSIONS

Data for a large number of materials tested in both a rotating disk device and a magnetostriction oscillator have been analyzed in a manner which brings the results of the two methods closer to a universal curve fit.

Normalized cumulative erosion rate has been plotted versus normalized time and a curve fit is proposed which covers a comprehensive variety of materials, test conditions, and devices. Cumulative erosion rate and time are normalized to the peak erosion rate and time to peak erosion rate, respectively. Adjustments are suggested for incubation periods.

It was shown that the universal approach plot is more accurate if small time intervals are used before the peak damage rate is reached.

After the peak damage rate is passed, at long exposure times, more resistant materials show a lower normalized average erosion rate.

The curves and data scatter bands derived from this universal curve-fit approach appear to be useful in correlating different types of laboratory tests with each other and with field data.

REFERENCES

(1) HONEGGER, E. Tests on erosion caused by jets. Brown Boveri Review, 1927, 14, 96-104.

(2) THIRUVENGADAM, A. and PREISER, H. S. On testing materials for cavitation damage resistance. Journal of Ship Research, 1964, 8, 39-56.

(3) PLESSET, M. S. and DEVINE, R. E. Effect of exposure time on cavitation damage. Journal of Basic Engineering, 1966, 88, 691-705.

(4) HEYMANN, F. J. On the time dependence of the rate of erosion due to impingement or cavitation. Erosion by Cavitation or Impingement. STP 408, American Society for Testing and Materials, Philadelphia, 1967.

(5) TICHLER, J. W. and DE GEE, A. W. J. Time dependence of cavitation erosion and the effect of some material properties. Proceedings 3rd International Conference on Rain Erosion and Associate Phenomena, Vol. 2, Royal Aircraft Establishment, Farnborough, 1970.

(6) THIRUVENGADAM, A. Handbook of Cavitation Damage. Hydronautics, Inc. Tech. Report 233-8, Laurel, Maryland, 1965.

(7) THIRUVENGADAM, A. Theory of erosion. Proceedings 2nd Meersburg Conference on Rain Erosion and Allied Phenomena, Vol. 2, Royal Aircraft Establishment, Farnborough, 1967.

(8) HOFF, G. and LANGBEIN, G. Resistance of materials towards various types of mechanical stress. Proceedings 2nd Meersburg Conference on Rain Erosion and Allied Phenomena, Royal Aircraft Establishment, Farnborough, 1967.

(9) HEYMANN, F. J. Toward quantitative prediction of liquid impact erosion. Characterization and Determination of Erosion Resistance, STP 474, American Society for Testing and Materials, Philadelphia, 1970.

(10) ENGEL, O. G. A first approach to a microscopic model of erosion rate in drop impact and cavitation. Proceedings 3rd International Conference on Rain Erosion and Associate Phenomena, Royal Aircraft Establishment, Farnborough, 1970.

(11) PERELMAN, R. G. and DENISOV, Y. D. The strength of materials under the action of droplet impacts. Royal Aircraft Establishment Library Translation No. 1654, 1971.

(12) LICHTAROWICZ, A. Cavitating jet apparatus for cavitation erosion testing. Erosion: Prevention and Useful Applications, STP 664, American Society for Testing and Materials, Philadelphia, 1979.

(13) MOSKIEVIC, J. Dyanamics of the cavitation damage. Proceedings, Joint Symposium on Design and Operation of Fluid Machinery, Vol. 2, Colorado State University Publications, Fort Collins, Colo., 1978.

(14) SCHMITT, G. F. Liquid and solid particle impact erosion. Wear Control Handbook, ASME, New York, 1980.

(15) ASTM Committee G2 Working Document. Standard practice for liquid impingement erosion testing. Draft no. 6, Mar. 1982.

(16) VEERABHADRA RAO, P. and YOUNG, S. G. Universal approach to analysis of cavitation and liquid-impingement erosion data. NASA TP-2061, 1982.

(17) VEERABHADRA RAO, P. Characteristics, correlations, similarities and prediction of erosion due to cavitation and liquid impingement. Ph.D Thesis, Indian Institute of Science, Bangalore, India, 1975.

(18) YOUNG, S. G. Cavitation damage of stainless steel, nickel and aluminum alloy in water for ASTM round robin tests. NASA TM X-1670, 1968.

(19) YOUNG, S. G. and JOHNSTON, J. R. Effect of temperature and pressure on cavitation damage in sodium. Characterization and Determination of Erosion Resistance, STP 474, American Society for Testing and Materials, Philadelphia, 1970.

(20) YOUNG, S. G. Study of cavitation damage to high purity metals and a nickel-base superalloy in water. NASA TN D-6014, 1970.

(21) VEERABHADRA RAO, P., SYAMALA RAO, B. C. and LAKSHMANA RAO, N. S. Erosion and cavity characteristics in rotating components. Journal of Testing and Evaluation, 1980, 8, 127-142.

(22) LAKSHMANA RAO, N. S., VEERABHADRA RAO, P. and SYAMALA RAO, B. C. A study of cavitation erosion in rotating components. Proceedings of 5th Conference on Fluid Machinery, Vol. I, Akademiai Kiado, Budapest, Hungary, 1975.

(23) KERR, S. L. Determination of the relative resistance to cavitation erosion by the vibratory method. Transactions of ASME, 1937, 59, 373-397.

(24) THOMAS, G. P. and BRUNTON, J. H. Drop impingement erosion of metals. Proceedings of Royal Society, London Series A, 1970, 314, 549-565.

(25) ELLIOTT, D. E., MARRIOTT, J. B. and SMITH, A. Comparison of erosion resistance of standard steam turbine blade and shield materials on four test rigs. Characterization and Determination of Erosion Resistance, STP 474, American Society for Testing and Materials, Philadelphia, 1970.

(26) Erosion by Cavitation and Impingement, STP 408, American Society for Testing and Materials, Philadelphia, 1967.

(27) Characterization and Determination of Erosion Resistance, STP 474, American Society for Testing and Materials, Philadelphia, 1970.

(28) THIRUVENGADAM, A. Erosion, Wear and Interfaces with Corrosion, STP 567, American Society for Testing and Materials, Philadelphia, 1974.

(29) ADLER, W. F. Erosion: Prevention and Useful Applications, STP 664, American Society for Testing and Materials, Philadelphia, 1979.

(30) HEYMANN, F. J. Conclusions from the ASTM interlaboratory test program with liquid impact erosion facilities. Proceedings 5th International Conference on Erosion by Solid and Liquid Impact, Cambridge University, Cambridge, England, 1979.

(31) SPINGER, G. S. Erosion by Liquid Impact, Scripta Publishing Company, Washington, D. C., 1976.

(32) VEERABHADRA RAO, P., et al. Estimation of cavitation erosion with incubation periods and material properties. Journal of Testing and Evaluation, 1981, 9, 189-197.

(33) McGUINESS, T. and THIRUVENGADAM, A. Cavitation erosion-corrosion modeling. Erosion, Wear and Interfaces with Corrosion, STP 567, American Society for Testing and Materials, Philadelphia, 1974.

Table 1 Predictive models, formulations, and parameters necessary for computation of cavitation and liquid-impingement-erosion-versus-time curves

Investigator	Type of erosion[a]	Parameters needed for computation
Thiruvengadam (6)	CAV (nomogram)	(1) Erosion intensity (2) Strain energy
Heymann (4)	CAV and LI (elementary model)	(1) Nominal mean lifetime for original surface (2) Standard deviation for original surface (3) Nominal mean lifetime for substructure (4) Standard deviation for substructure
	LI (elaborated model)	(1) Delay time during which no failure occurs (2) Mean of log-normal distribution on logarithmic time scale (3) Standard deviation of log-normal distribution on logarithmic time scale
Thiruvengadam (7)	LI and CAV	(1) Magnitude of instantaneous erosion rate at first peak (2) Time to attain first peak instantaneous erosion rate (3) Attenuation exponent (4) Weibull shape parameter
Hoff and Langbein (8)	LI (rain erosion)	(1) Maximum rate of erosion (2) Incubation period (intercept on time axis from straight-line portion of erosion-versus-time curve)
Heymann (9)	CAV and LI	(1) Mean depth of erosion at tangent point (2) Average erosion rate at tangent point (3) Exponential constant
	LI	(1) Cumulative mean depth of erosion or material loss at tangent point (2) Normal component of impact velocity (3) Volume of liquid impinging per unit area per unit time (4) Generalized nondimensional erosion resistance parameter
Tichler and deSee (5)	CAV	(1) Incubation time (2) Resistance against cavitation erosion under hydrodynamic conditions, as occur in magnetostrictive oscillator (3) Mean depth of erosion at which effect of crater formation becomes manifest (4) Proportionality constant, symbolizing increase in mean depth of erosion that would be necessary to form number of craters per unit area in final steady-state period (5) Ratio of rate of erosion in final steady-state period to rate of erosion in first steady-state period
Perelman and Denisov (11)	LI	(1) Work done on microplastic deformations per cycle of load, due to the energy capacity of microvolumes of the material (2) Energy expended on fatigue fracture (3) Influence of the surface form (4) Kinetic energy of a stream of droplets (5) Energy in a stream of droplets absorbed during the incubation period (6) Specific energy of fracture determined from macroscopic fracture tests (7) Energy absorbed by the material during initial deformation
Lichtarowicz (12)	LI (graph)	(1) Cumulative peak erosion rate (2) Time to reach cumulative peak erosion rate
Hoskievic (13)	CAV	(1) Cavitation property of material (2) Cavitation strength of material or inner friction of material during plastic deformation (3) Cavitation damage rate in developed period of cavitation attack
Thiruvengadam (14)	CAV and LI (nomogram)	(1) Erosion intensity (2) Erosion strength
Rao and Young (16)	CAV and LI	(1) Peak cumulative average erosion rate (2) Time to attain peak cumulative average erosion rate (3) Incubation period (4) Erosion resistance

[a] CAV: Cavitation erosion.
LI: Liquid impingement erosion, cylindrical/spherical drop or jet impact including jet with cavitation inducer.

Table 2 Maximum rate of erosion and the impacts to attain it for various materials - drop impact

[Drop size, 1.5 mm; velocity, 125 m/sec; data source, (24).]

Material	Maximum rate of erosion, μm/impact		$\frac{MER_i}{MER_a}$	Impacts to attain maximum erosion rate		$\frac{tm_i}{tm_a}$
	Instantaneous, MER_i	Average, MER_a		Instantaneous, tm_i	Average, tm_a	
Cobalt	0.93×10^{-3}	0.37×10^{-3}	2.52	5.07×10^5	7.4×10^5	0.69
18/8 stainless steel	2.86	.89	3.21	3.51	4.78	.74
Copper	8.85	6.21	1.43	.3	.38	.80
Mild steel		1.74			3.05	
60/40 brass	4.92	1.81	2.73	3	3.76	.80
Silicon steel	4.33	1.52	2.84	3.51	4.28	.82

Table 3 Maximum rate of erosion and time to attain it for L-605 cobalt alloy in a magnetostriction apparatus with small and large intervals of time

[Data source, (19), test liquid, liquid sodium at 427° C; amplitude, 44.5 μm; frequency, 25 kHz; specimen, vibrating.]

Pressure, MPa	Maximum rate of erosion, mm^3/hr				Time to attain maximum rate of erosion, min			
	Small intervals, 5 and 10 min		Long intervals, 60 min		Small intervals, 5 to 10 min		Long intervals, 60 min	
	Instantaneous, MER_i	Average, MER_a	Instantaneous, MER_i	Average, MER_a	Instantaneous, tm_i	Average, tm_a	Instantaneous, tm_i	Average, tm_a
0.2	22.80	14.22	16.62	12.96	75	120	90	80
.3	42.78	33.60	31.80	31.80	22.5	45	[a]30	[a]60
.4	85.80	88.20	46.62	46.62	10	15	[a]30	[a]60

[a]Minimum calculation time possible when calculated by this method.

Table 4 Prediction of erosion using normalized average erosion rate and instantaneous erosion rate

Rig	MER_i, mg/kg	tm_i, kg/cm^2	$\frac{ER}{MER_i}$	Percent error of normalized erosion rate	MER_a, mg/kg	tm_a, kg/cm^2	$\frac{ER}{MER_a}$	Percent error of normalized erosion rate
EEC[a]	193	1.6	0.19	0	119	1.28	0.67	0
CAP[b]	2.46	22.4	.25	32	1.54	41.04	.97	45
Rapier[c]	92.8	3.8	.34	79	41	6.05	.81	21

[a]EEC - The English Electric Company rig.
[b]CAP - The C. A. Parsons' erosion rig.
[c]Rapier - The Rapier erosion test rig of the Central Electricity Generating Board (CEGB).

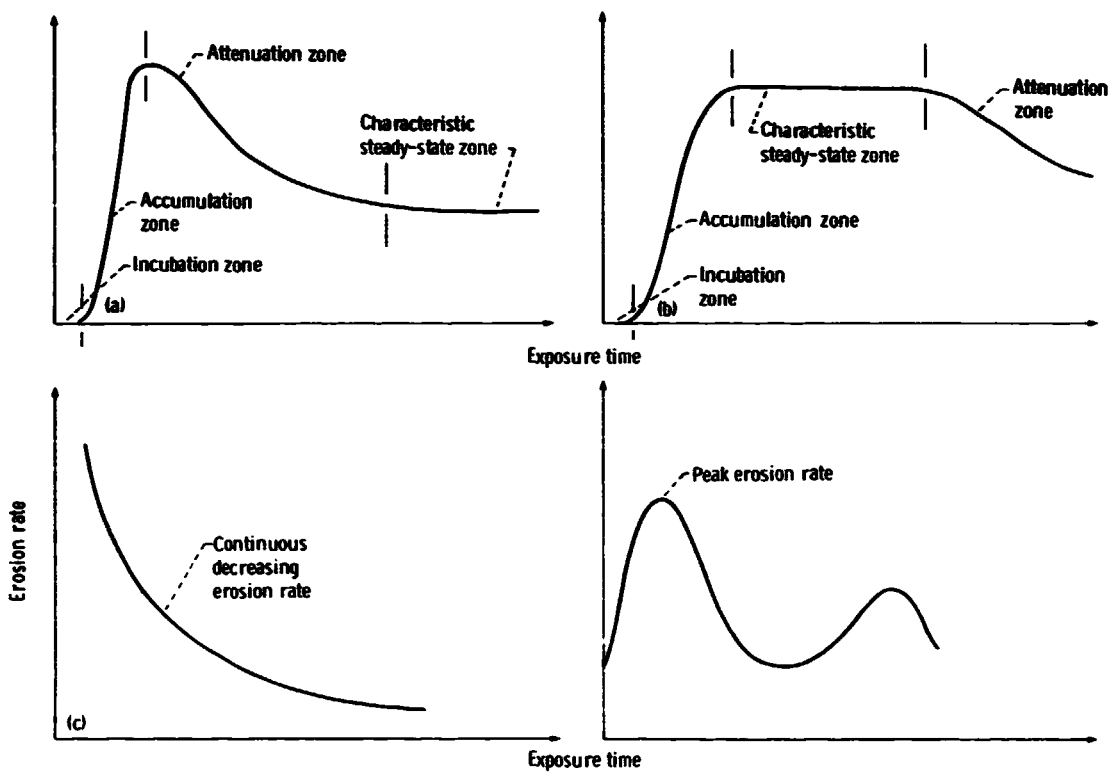

(a) Thiruvengadam and Preiser (2). (b) Plesset and Devine (3).

(c) Heymann (4). (d) Tichler and de Gee (5).

Figure 1. - Characteristic erosion-rate-versus-time curves.

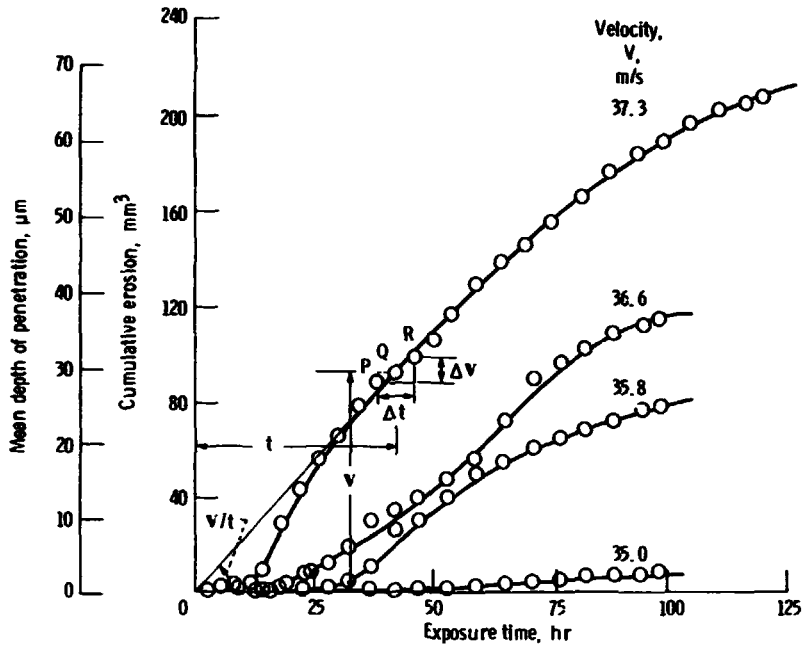

Figure 2. - Cumulative erosion versus time for stainless steel tested in rotating-disk device. Pressure, 150 kPa abs; inducer diameter, 25.4 mm. Instantaneous erosion rate at Q equals slope of local tangent at Q = $\Delta V/\Delta t$; cumulative average erosion rate at Q equals slope of line joining origin and point Q = V/t.

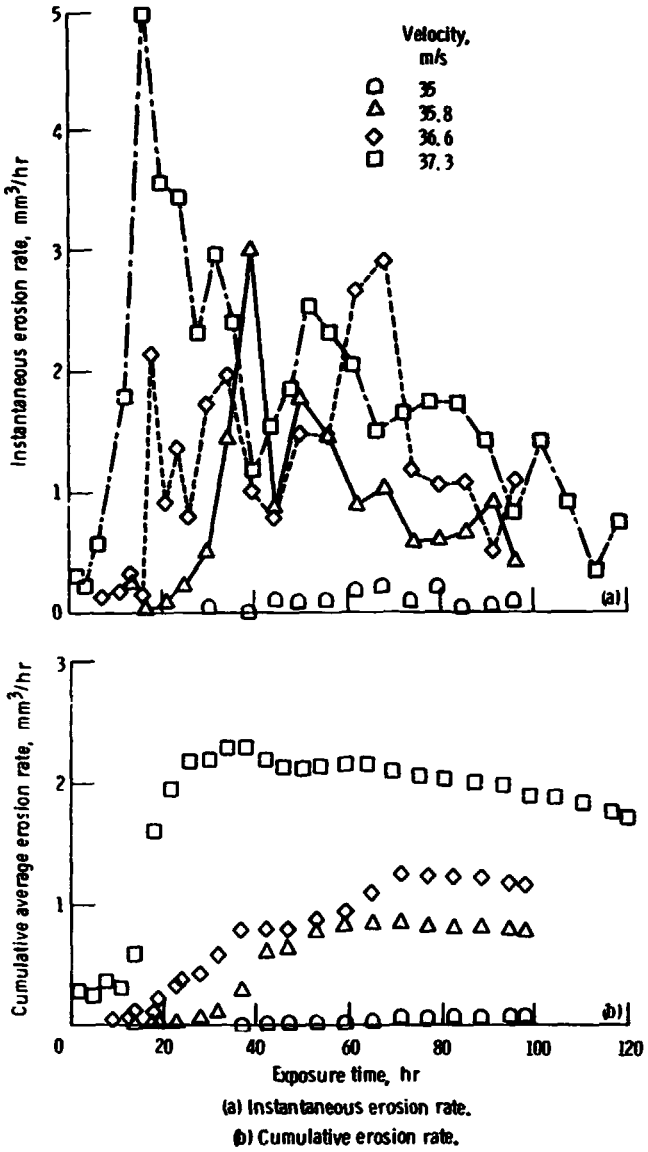

(a) Instantaneous erosion rate.

(b) Cumulative erosion rate.

Figure 3. - Erosion rate versus time for stainless steel tested in a rotating disk device at various velocities. Pressure, 0.150 MPa abs.

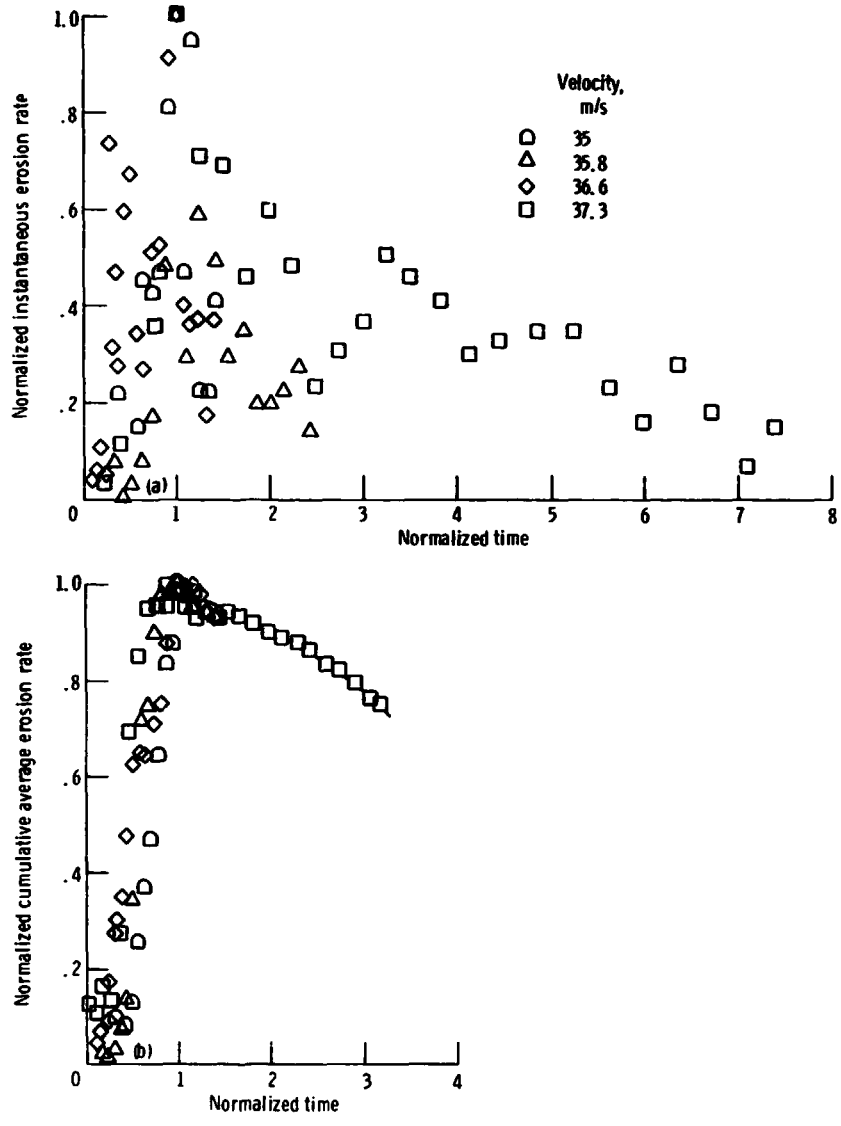

(a) Instantaneous erosion rate.

(b) Cumulative erosion rate.

Figure 4. - Normalized erosion rate versus normalized time for stainless steel tested in a rotating disk device at various velocities. Pressure, 0.150 MPa abs.

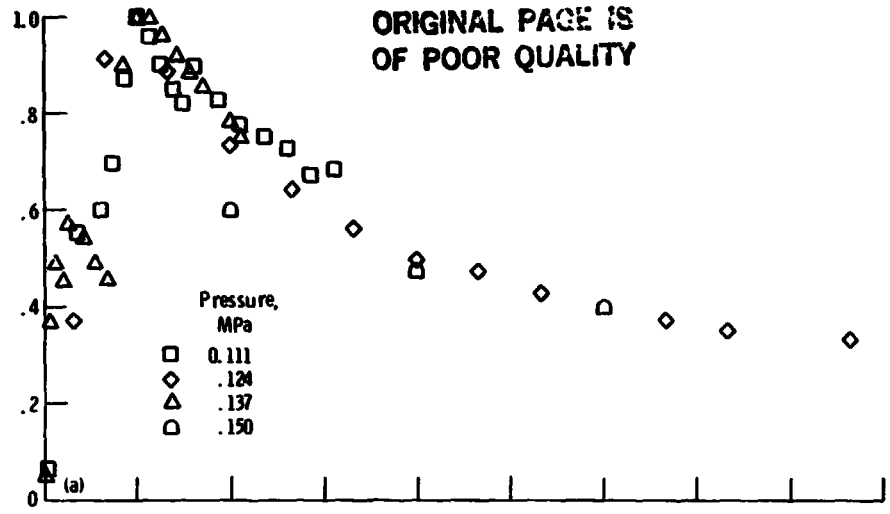

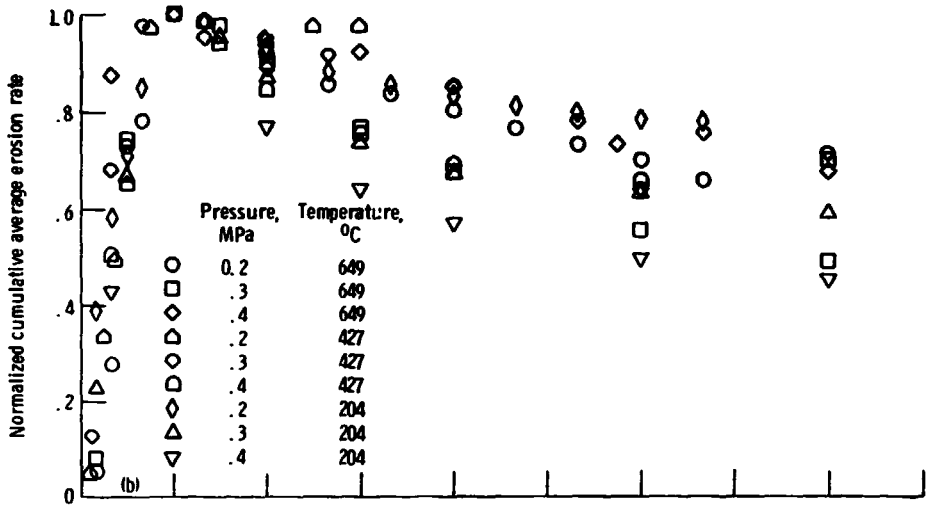

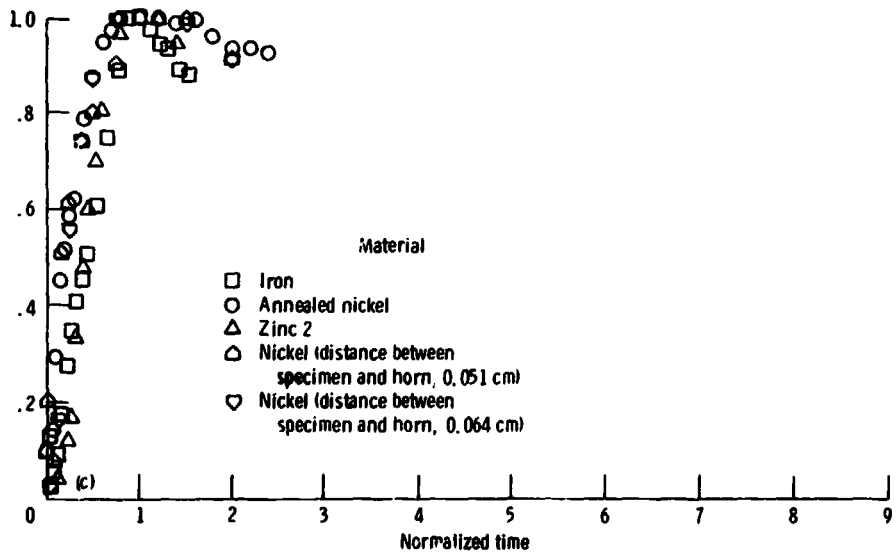

(a) Aluminum tested with a rotating disk device Velocity, 35.8 m/s; temperature, $32^0 \pm 2^0$ C; test liquid, water.

(b) L-605 cobalt alloy tested with a magnetostriction apparatus. Specimen, vibrating; frequency, 25 kHz; test liquid, liquid sodium.

(c) Various materials tested with a magnetostriction apparatus. Specimen, stationary; frequency, 25 kHz; pressure, 10^5 Pa; room temperature; test liquid, water.

Figure 5. - Normalized average erosion rate versus normalized time for various materials tested.

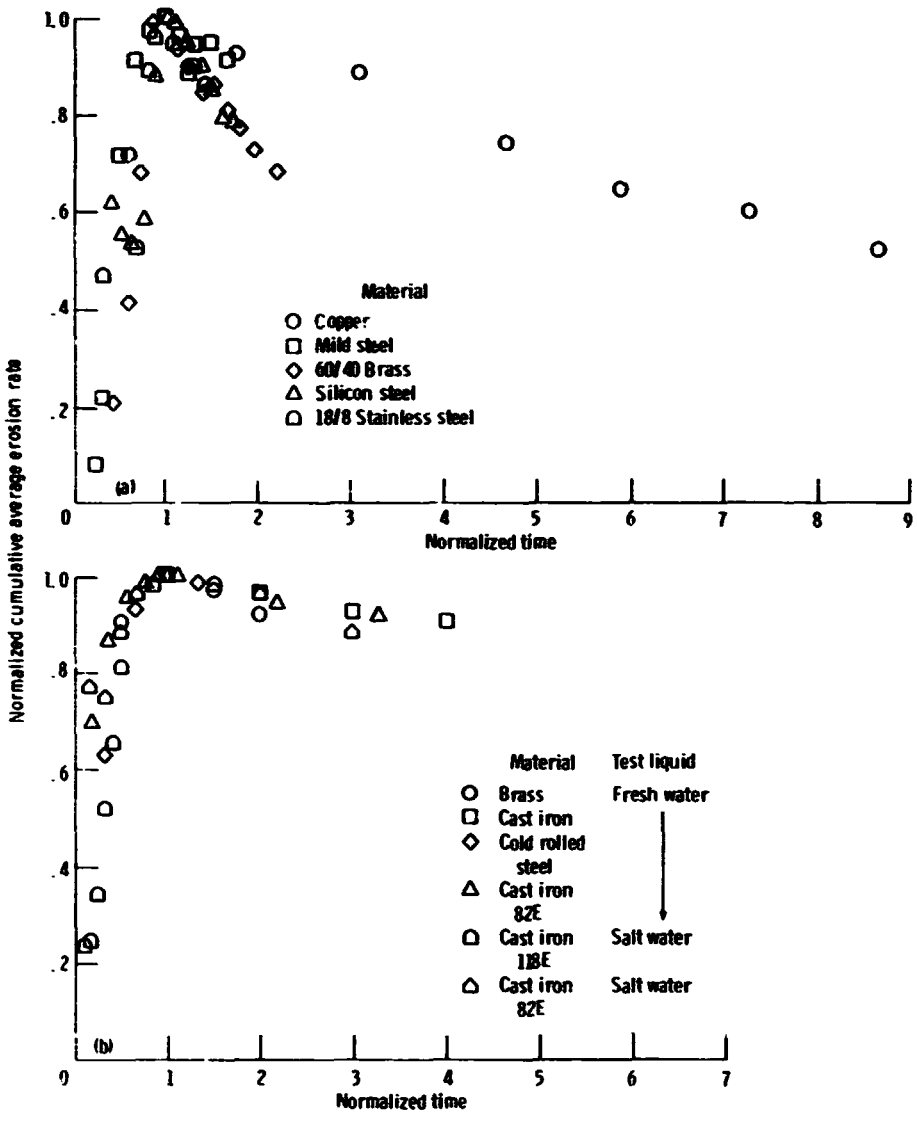

(a) Liquid impingement (data from (24)).

(b) Vibratory cavitation (data from (23)).

Figure 6. - Normalized average erosion rate versus normalized time for various materials tested.

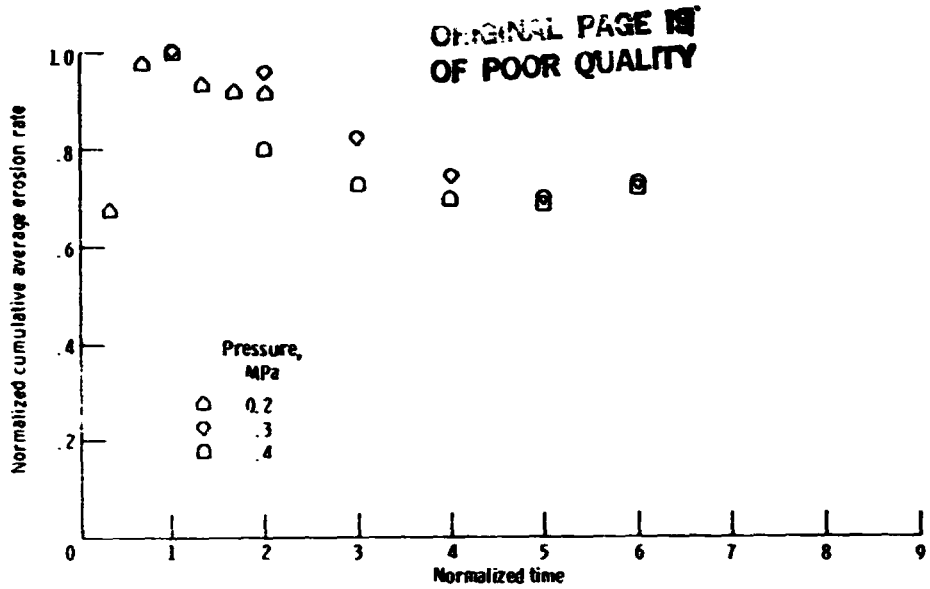

Figure 7. - Normalized erosion rate versus normalized time for L-605 alloy tested in magnetostriction apparatus at 427° C in liquid sodium; 1-hr time intervals; specimen, vibrating; frequency, 25 kHz.

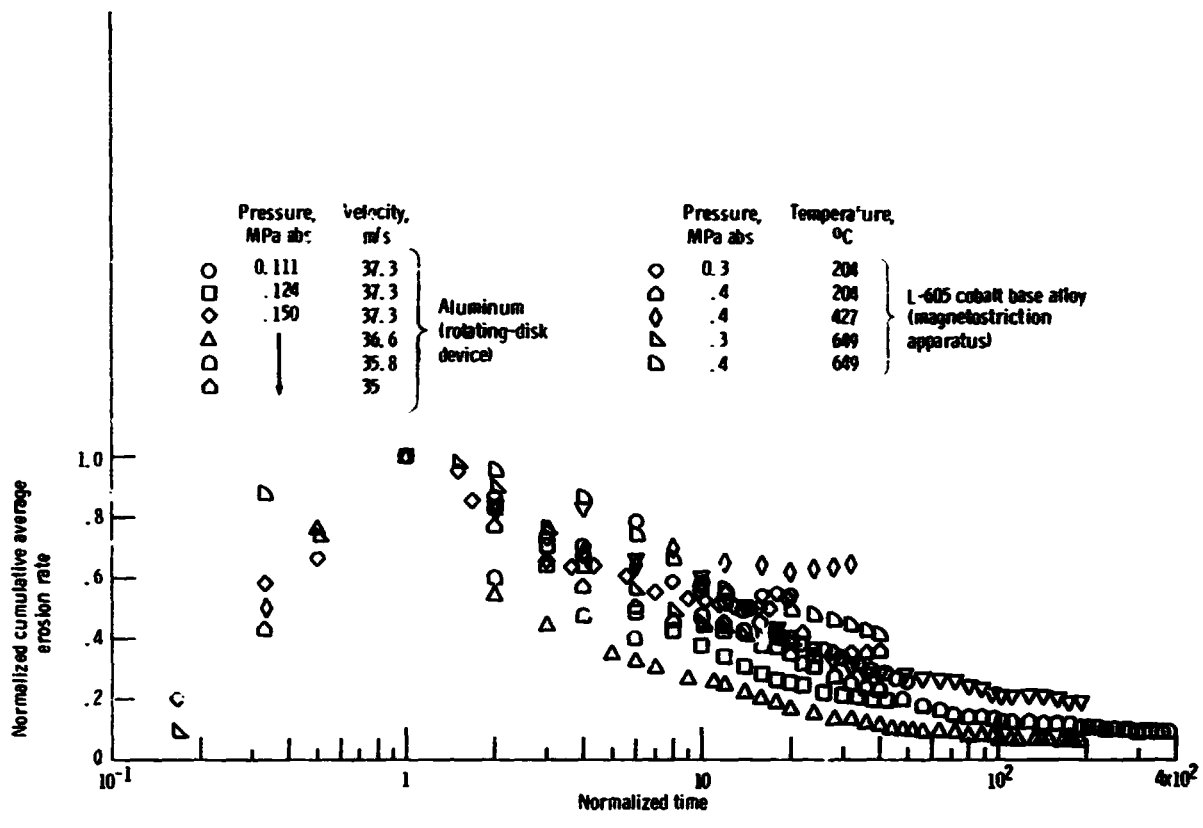

Figure 8. - Normalized cumulative average erosion rate versus normalized time for long exposures.

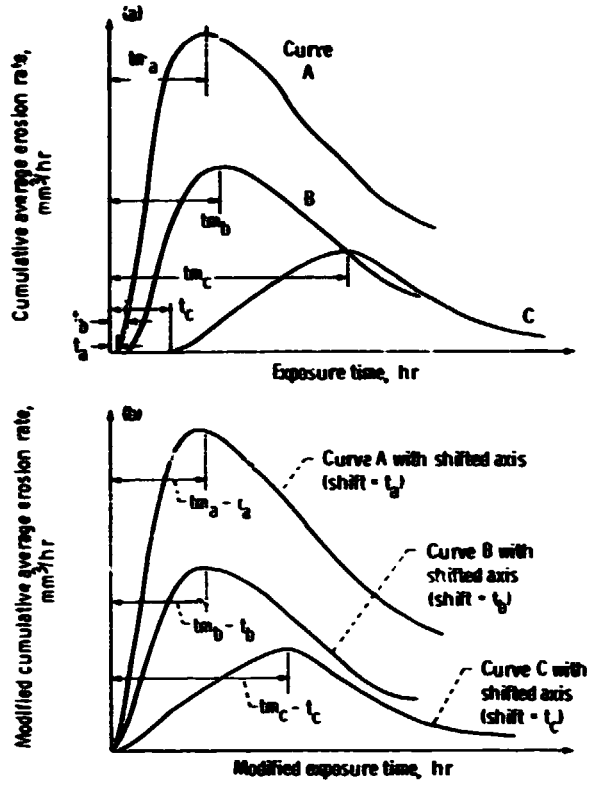

(a) Typical cumulative-average-erosion-rate-versus-time curves.

(b) Modified cumulative-average-erosion-rate-versus-modified-time curves.

Figure 9. - Effect of incubation period correction where t_a, t_b, and t_c denote the incubation periods of curves A, B, and C, respectively, and tm_a, tm_b, and tm_c denote times to attain maximum rates of erosion of curves A, B, and C, respectively.

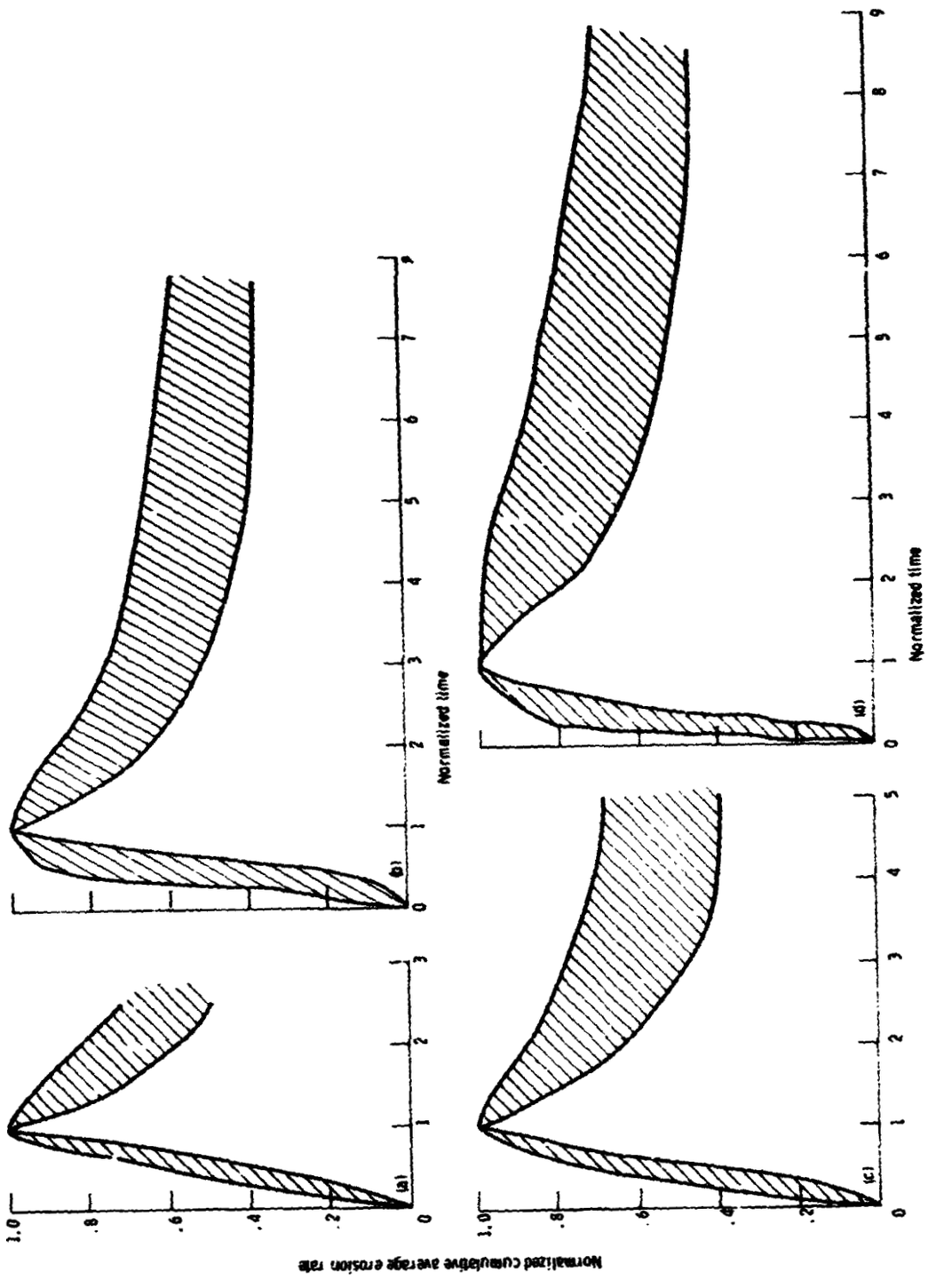

(a) Brass.
(b) Stainless steel.
(c) Mild steel.
(d) L-605 cobalt-base alloy.

Figure 10. - Summary plots for brass, stainless steel, mild steel, and L-605 cobalt-base alloy.